

1 **The influences of different substituents on spectral properties of**  
2 **Rhodamine B based chemosensors for mercury ion and application in**  
3 **EC109 cells**

4  
5 Wenqi Du<sup>[a]</sup>, Yu Cheng<sup>[a]</sup>, Weixin Shu<sup>[a]</sup>, Baoying Wu<sup>[a]</sup>, Zhineng Kong<sup>[a]</sup>, Zhengjian  
6 Qi<sup>\*[a]</sup>

7  
8 <sup>[a]</sup>College of Chemistry and Chemical Engineering, Southeast University Road 2,  
9 Jiangning District 211189, Nanjing, Jiangsu Province, P.R. China

10  
11 Email: qizhengjian506@163.com

12 \*For correspondence

13

14 **Abstract:** Six rhodamine-based “Turn-on” fluorescence chemosensors(L<sub>1-6</sub>) with  
15 different substituents for Hg<sup>2+</sup> were readily synthesized and investigated, which  
16 displayed high selectivity and chelation enhanced ratiometric fluorescence change and  
17 colorimetric change with Hg<sup>2+</sup> among the metal ions examined. Based on UV spectral  
18 data and fluorescence spectral data, the effect of different substituents on spectral  
19 properties of the probes were presented and discussed. The detection limit of Hg<sup>2+</sup> to  
20 probe L<sub>1</sub> was as low as 50 nM, which attribute to its electron donating group.  
21 Theoretical calculation also support the process of reaction. Confocal laser scanning  
22 microscopy experiments showed that probe could be used to detect Hg<sup>2+</sup> in living  
23 cells.

24  
25 **Keywords:** Rhodamine B; Fluorescent chemosensor ; Sensing mercury ion; Living  
26 cells.

## 27 28 1.Introduction

29 Various transition-metal ions are essential to the life of creatures. Mercury is a  
30 dangerous and hazardous toxic which has posed a great threat to our environment<sup>1-4</sup>.  
31 Mercury is heavy metal, which can be dispersed in the atmosphere, the ocean, and  
32 the soil. Different speciation mercury can penetrate our environment by various ways,  
33 such as methyl mercury produced by aquatic microbes which bioaccumulates  
34 through the food chain and oxidation of mercury vapor in atmosphere to  
35 water-soluble Hg<sup>2+</sup> ions<sup>5-7</sup>. After long-term exposure in the environment, mercury ion  
36 accumulate in organisms which can cause nausea, vomiting, abdominal pain, renal  
37 dysfunction and other diseases.

38 At present, UV spectrophotometry, electrochemical methods, ionization coupled  
39 plasma mass spectrometry, ionization coupled plasma atomic emission spectrometry,  
40 atomic absorption spectroscopy and other analytical methods can be used to identify  
41 and detect metal ions<sup>8-12</sup>. However, these methods have some disadvantages in the  
42 application, such as high detection costs, narrow range of applications, and can't  
43 achieve real-time detection. In contrast, the fluorescent molecular probe has no

44 damage to the sample, and gives its priority to easy operability and high sensitivity,  
45 so fluorescence analytical methods are effective and efficient ways to detect ions<sup>13-15</sup>.

46 Compared with other fluorescent dyes, rhodamine dyes have some excellent  
47 photophysical properties, such as high fluorescence quantum yield, pH insensitive,  
48 high molar absorptivity and high extinction coefficient, particularly in its nucleotide  
49 and nucleic acid conjugates<sup>16</sup>. Some rhodamine-based chemosensors for Hg<sup>2+</sup> ions  
50 have been reported<sup>17-22</sup>, but dual colorimetric and fluorescent chemosensors for  
51 mercury ion were still rare<sup>23</sup> and some of them were not efficient enough to be  
52 selective toward mercury ion.

53 Here, we report six rhodamine-based caprolactam derivatives as a sensor for  
54 Hg<sup>2+</sup>, when binding phenomena could be probed through binding-induced changes in  
55 an electronic spectral pattern. The difference between these probes are that we  
56 selected different substitutional group such as methyl group, nitro group, aldehyde  
57 group, halogen group, phenyl group. These rhodamine-based derivatives that  
58 behaves as a fluorescent Hg<sup>2+</sup> sensor with high emission sensitivity and selectivity,  
59 which exhibited sensitive detection toward Hg<sup>2+</sup> via significant fluorescence  
60 enhancement in solution, and in the meantime they showed a significant color  
61 change from colorless to rose red. We have designed some similar structures to  
62 compounds L<sub>1-6</sub> and conduct a series of experiments to explore their properties  
63 which have the correlations of nature of substituent group. After comparison of  
64 optical properties, probe L<sub>1</sub> showed a good performance in the recognition toward  
65 Hg<sup>2+</sup>, which indicated that the different electronic distribution among the sensors'  
66 structures make an influence on their properties. For this reason, we selected L<sub>1</sub> as a  
67 typical example to expound in the following discussion.

## 68 **2. Experimental**

### 69 **2.1 Apparatus and Materials**

70 Fluorescence spectra measurement were performed on Horiba Jobin Yvon Inc.  
71 Fluorolog 3-TSCPC. <sup>1</sup>H NMR spectrum was run on a Bruker 300 MHz spectrometer  
72 using TMS as the internal standard. Mass spectrum was recorded with a VG ZAB-HS  
73 double focusing mass spectrometer. Absorption spectra were measured on a UV-2201

74 double-beam UV/VIS spectrometer. Melting point was determined using an SGW X-4  
75 digital melting point apparatus.

76 All the materials for synthesis were purchased from Sinopharm Chemical Reagent  
77 Co.,Ltd (Shanghai, China) and used without further purification. Metal solutions  
78 were prepared from their analytical grade nitrate salts. The metal ions were prepared  
79 as 0.2 mM in water solution.

## 80 2.2 Syntheses

81 As shown in Scheme 1, the compounds L<sub>1</sub>~L<sub>6</sub> were prepared by reacting RBH with  
82 aromatic aldehyde. RBH was synthesized according to literature.

### 83 2.2.1 Synthesis of RBH

84 As for the synthesis of RBH, several different procedures have been reported<sup>24-26</sup>.  
85 In this work, RBH was synthesized by a modified method according to Xiang<sup>27</sup>. m/z:  
86 457.2265 ([M+H]<sup>+</sup>); M<sup>+</sup> calculated 456.2265. IR(KBr,cm<sup>-1</sup>):  $\nu$  = 3428, 2987, 2926,  
87 1689, 1614, 1514, 1380, 1218, 1117, 818, 767. <sup>1</sup>H NMR (300 MHz, CDCl<sub>3</sub>,  $\delta$  ppm),  $\delta$   
88 (ppm):1.17 (t, 12H), 3.34 (q, 8H), 3.62 (bs, 2H), 6.29 (dd, 2H), 6.43(d, 2H),6.45 (d,  
89 2H), 7.11 (dd, 1H), 7.42 (d, 1H), 7.44(d, 1H), 7.93 (dd, 1H). (Fig.S1~S3)

### 90 2.2.2 Synthesis of L<sub>1</sub>

91 RBH ( 0.5 mmol, 0.24 g) was dissolved in 30 mL ethanol, and then p-tolualdehyde  
92 (0.5 mmol, 0.12 g) was slowly added. The mixture was stirred and refluxed for 12 h  
93 at 80 °C. After distillation in vacuum, the residue was recrystallized with methanol  
94 and water to give the final product L1 in yield of 79.8%. m/z: 559.3020([M+H]<sup>+</sup>);  
95 M<sup>+</sup>calculated 558.3020. <sup>1</sup>H NMR (300 MHz, CDCl<sub>3</sub>,  $\delta$  ppm): 8.64 (s, 1H),7.97 (m,  
96 1H), 7.49 (d, 2H), 7.45 (m, 2H),7.26 (d, 1H), 7.09 (m, 2H), 6.54 (d, 2H), 6.43 (s, 2H),  
97 6.26 (d, 2H), 3.33 (q, 8H), 2.29 (s, 3H), 1.15(t, 12H). (Fig.S4~S6)

### 98 2.2.3 Synthesis of L<sub>2-6</sub>

99 Compound L<sub>2-6</sub> was prepared using a general procedure which is essentially similar  
100 to that used for L<sub>1</sub>. (Fig.S7~S21)

## 101 3. Results and Discussion

102 The structure of compounds L<sub>1-6</sub> were characterized by <sup>1</sup>H NMR, HR-MS. The  
103 results were in good agreement with the structure showed in Scheme 1. Fluorescence

104 and UV–vis studies were performed using a 20  $\mu\text{M}$  solution of  $\text{L}_{1-6}$  in a  $\text{CH}_3\text{CN}/\text{H}_2\text{O}$   
105 (1:1, v/v) solution with appropriate amounts of metal ions.

### 106 3.1 Comparison of six rhodamine B based sensors

107 Under the same conditions, we explore the sensitivity measurement of ion probes.  
108 As shown in Fig.1, rhodamine B derivatives with methyl exhibits excellent sensitivity  
109 towards mercury ion. Derivatives with halogen group also show good sensitivity  
110 owing to its electron donating groups. Based on these phenomena, it suggested that  
111 chelation-enhanced fluorescence appears when compounds with electron donating  
112 groups are complexed with  $\text{Hg}^{2+}$ . In order to further explore the affinity capacity  
113 between probes and metal ions, association constants were calculated to verify the  
114 experiment we have conducted. It is indicated in the Scheme 2, the numerical size of  
115 association constants diminished in order, which in accordance with the results of  
116 fluorescence intensity when different substituents with rhodamine B binds to mercury.

117 After comparison between these probes, we can come to conclude that methyl  
118 group, halogen group and phenyl group belong to electron donating group while nitro  
119 group, aldehyde group belong to electron-attracting group. When interacting with  
120 mercury ion, electron donating group provide electron to coordination site which  
121 make it easier to combine. On the contrary, electron-attracting group make it more  
122 difficult for probe to interact with mercury ion. So, we prefer to select electron  
123 withdrawing substituents to detect metal ions which reveals high sensitivity. To  
124 investigate photoelectric properties of these probes further, we selected  $\text{L}_1$  as an  
125 typical example to expound in the discussion.

### 126 3.2 Metal ion selectivity and competition experiments

127 As shown in Fig.2, UV–vis spectrum of compound  $\text{L}_1$  (20 $\mu\text{M}$ ) exhibited only very  
128 weak bands over 450 nm, which could be attributed to the presence of a trace amount  
129 of the ring-opened form of compounds. On addition of 10 equiv.  $\text{Hg}^{2+}$  into solution,  
130  $\text{L}_1$  immediately resulted in a significant enhancement of absorbance at about 556 nm  
131 simultaneously the color changed into rose red. Other metal ions such as  $\text{Zn}^{2+}$ ,  $\text{Mg}^{2+}$ ,  
132  $\text{Ca}^{2+}$ ,  $\text{Cd}^{2+}$ ,  $\text{Cu}^{2+}$ ,  $\text{Pb}^{2+}$ ,  $\text{Ba}^{2+}$ ,  $\text{Ni}^{2+}$ ,  $\text{Mn}^{2+}$ ,  $\text{K}^+$ ,  $\text{Li}^+$ ,  $\text{Ag}^+$ ,  $\text{Co}^{2+}$ , except for  $\text{Fe}^{3+}$ , did not  
133 show any significant color and spectral change under any significant color and

134 spectral change under identical conditions. These phenomena suggest that these  
 135 compounds can serve as a “naked-eye” chemosensor for Hg<sup>2+</sup>. To further investigate  
 136 the interaction of Hg<sup>2+</sup> and the probe, the Hg<sup>2+</sup> binding stoichiometry of the probe can  
 137 be determined from titration and the Job plot<sup>28,29</sup>. As shown in Fig.3, it is obvious that  
 138 the fluorescence intensity reached a maximum when the ratio was 0.5, which  
 139 suggesting that a 1:1 stoichiometry of the Hg<sup>2+</sup> to the probes respectively in the  
 140 complex. Furthermore, we also conducted the competitive experiments which  
 141 indicates the background metal ions showed very low interference with the detection  
 142 of Hg<sup>2+</sup> in the water solutions (Fig.4.).

### 143 3.3 Emission spectra and detection limit of sensor

144 A fluorescence titration experiment was carried out in order to further explore the  
 145 interaction of probes and Hg<sup>2+</sup>. On addition and gradual increase concentration of  
 146 mercury ions to the L<sub>1</sub> in CH<sub>3</sub>CN/H<sub>2</sub>O(V:V=1: 1), the fluorescence intensity gradually  
 147 increased and the solutions turned colorless to rose red. Limit detection of metal ions  
 148 plays an important role in evaluating fluorescence chemosensor. As for probe L<sub>1</sub>, the  
 149 linear response for the fluorescence intensity response of compound L<sub>1</sub> was between 0  
 150 and 140 μM (Fig. 5), and the detection limit of Hg<sup>2+</sup> was measured to be 0.05 μM.  
 151 The association constant K of the complex L<sub>1</sub>-Hg<sup>2+</sup> was then calculated to be  
 152 3.24×10<sup>3</sup> M<sup>-1</sup> with a linear relationship (Fig. 6) by Benesi–Hildebrand method, Eq.  
 153 (1)<sup>30, 31</sup>

$$154 \quad \frac{1}{F - F_0} = \frac{1}{K(F_{Max} - F_{Min})[Hg^{2+}]} + \frac{1}{F_{Max} - F_{Min}} \quad (1)$$

155 As shown in the Fig.7, probe L<sub>1</sub> show a weak fluorescence in the absence of metal  
 156 ions. On the addition of 10 equiv. metal ions, the fluorescence intensity has changed. It  
 157 is obvious that when 10 equiv. Hg<sup>2+</sup> was introduced into a solution of L<sub>1</sub> in  
 158 CH<sub>3</sub>CN/H<sub>2</sub>O (1:1, v/v), the fluorescence intensity increased sharply. Under this  
 159 conditions, Fe<sup>3+</sup> induce a mild fluorescence enhancement while Zn<sup>2+</sup>, Mg<sup>2+</sup>, Ca<sup>2+</sup>,  
 160 Cd<sup>2+</sup>, Cu<sup>2+</sup>, Pb<sup>2+</sup>, Ba<sup>2+</sup>, Ni<sup>2+</sup>, Mn<sup>2+</sup>, K<sup>+</sup>, Li<sup>+</sup>, Ag<sup>+</sup>, Al<sup>3+</sup>, Co<sup>2+</sup> and Na<sup>+</sup> did not show  
 161 remarkable changes in fluorescence intensity and the color.

### 162 3.4 Time-dependence and Fluorescent lifetime

163 Time-dependence for binding of the probe  $L_1$  with  $Hg^{2+}$  is given in Fig.8.  
164 Following the addition of 10 equiv.  $Hg^{2+}$  ion to 20.0  $\mu M$  probe  $L_1$ , the fluorescence  
165 intensity of probe  $L_1$  was turned on rapidly and reached a stable value within 2 min.  
166 The fluorescence lifetime was measured at an excitation 460 nm of the NanoLED  
167 source. The decays of probes were found to be monoexponential. The lifetime decays  
168 in the absence of  $Hg^{2+}$  and in the presence of  $Hg^{2+}$  are shown in Fig.9. The average  
169 lifetime of  $L_1$  was 1.87 ns and 5.00 ns (XSQ = 1.06) while the lifetime of  $L_1 + Hg^{2+}$   
170 was 1.91 ns (XSQ = 1.14). Double exponential fitting equation was used to describe  
171 the fluorescence lifetime of probe itself, because xanthene was a chromophore which  
172 formed a conjugated system. The upper part of structure formed a plane and  
173 orthogonalized with the ring of xanthene which also can be seen as a chromophore.  
174 After adding metal ions, the upper part including carbonyl group and phenyl group do  
175 not conjugate with xanthene, and the stereo-hindrance effect of carbonyl group limits  
176 the rotation of the benzene ring. So the major chromophore is still xanthene which  
177 used single exponential fitting equation.

### 178 3.5 Application

#### 179 3.5.1 Test papers

180 To demonstrate the practical application of our sensor, we prepared the test papers  
181 of sensor  $L_1$ . As depicted in Fig.10, the color of the test paper changed from colorless  
182 to purple and deepened gradually with the increasing of  $Hg^{2+}$  concentration. These  
183 paper-made test kits may be used as a simple tool for detecting  $Hg^{2+}$  in environmental  
184 samples.

#### 185 3.5.2 Fluorescence imaging for EC109 cells

186 Owing to its favourable spectroscopic properties of the response to  $Hg^{2+}$ ,  $L_1$  should  
187 be suited for fluorescence imaging in living cells. Laser scanning confocal  
188 microscopy was used to investigate this proposition. As determined by laser  
189 scanning confocal microscope, EC109 cells with a 10  $\mu M$  solution of probe  $L_1$  in  
190  $CH_3CN-H_2O$  (1:1, v/v) 30 min at 25 °C led to no intracellular fluorescence (Fig.11b.).  
191 After washed with PBS three times, the staining cells were then supplemented with 10  
192  $\mu M$  of  $Hg^{2+}$  under the same condition for 30 min, a significant increase of

193 fluorescence from the intracellular area was observed ( Fig.11c).

### 194 3.6 Mechanism

195 To investigate the interaction of probes and metal ions, probe L<sub>1</sub> was selected as an  
196 example to explain mechanism. IR spectra of L<sub>1</sub> and L<sub>1</sub>+Hg<sup>2+</sup> were taken in KBr disks  
197 (Fig.S22). It can be seen that the peak at 1698 cm<sup>-1</sup> which relates to the amide  
198 carbonyl absorption disappeared upon with the addition of Hg<sup>2+</sup>. To further  
199 investigate the mechanism of the reaction,we selected L<sub>1</sub> as an typical example to  
200 explain the phenomena. In addition, EDTA-adding experiment has been conducted to  
201 confirm the reversibility of reaction and the result was shown in the Fig.12,when the  
202 30 equiv. EDTA was added into L<sub>1</sub>+ Hg<sup>2+</sup> in CH<sub>3</sub>CN/H<sub>2</sub>O solution, the fluorescence  
203 intensity was decreased rapidly(green line).Then after adding the 30 equiv. Hg<sup>2+</sup>, the  
204 fluorescence intensity was recovered (red line) . This phenomenon indicates that the  
205 reaction between the compound and the metal ion are reversible.

206 As shown in the Fig.13, it indicates that these sereval chemosenors exhibit  
207 reversible and sensitive detection to Hg<sup>2+</sup>. While hydrolytic action of compounds  
208 might be happen after a long-term interaction with metal ions. Theoretical calculation  
209 has been conducted to verify the stability of compound L<sub>7</sub>, we assume the structure L<sub>7</sub>  
210 was existed after interacting with Hg<sup>2+</sup>. Frequency calculation successfully provide  
211 the evidence for the existence of the stable structure. To investigate the possible  
212 mechanism of the absorption and fluorescent emission of L<sub>1</sub>, theoretical calculation of  
213 L<sub>1</sub> which based on the optimized structures of the ground S<sub>0</sub> state and the first  
214 excited S<sub>1</sub> state were performed in Fig.14. After adding Hg<sup>2+</sup>, the energy gap between  
215 the HOMO and LUMO is greatly decreased<sup>32</sup>.

### 216 4. Conclusions

217 In summary, we reported the design and synthesis of six new rhodamine-based  
218 derivatives L<sub>1-6</sub> used as sensitive and selective chemosenor, which could specifically  
219 recognize Hg<sup>2+</sup> ion in solutions by naked eyes. These six probe display 1:1 complex  
220 formation with Hg<sup>2+</sup> which could be monitored by the spectral changes as well as  
221 color changes. Based on the experiment above, after a series comparison of these  
222 probes with different substituent group, L<sub>1</sub> shows better optical properties than others

223 owing to its electron donating group and excellent properties. Confocal laser scanning  
224 microscopy experiments showed that L<sub>1</sub> could be used to detect Hg<sup>2+</sup> in living cells.  
225 Furthermore, these six new probes show a great potential for biotic environmental  
226 detection.

### 227 **Supplementary Information (SI)**

228 The structure of compounds RBH, L<sub>1-6</sub> were characterized by <sup>1</sup>H NMR, HR-MS, IR in  
229 Supplementary Information. Supplementary Information is available at  
230 [www.ias.ac.in/chemsci](http://www.ias.ac.in/chemsci).

231

### 232 **Acknowledgements**

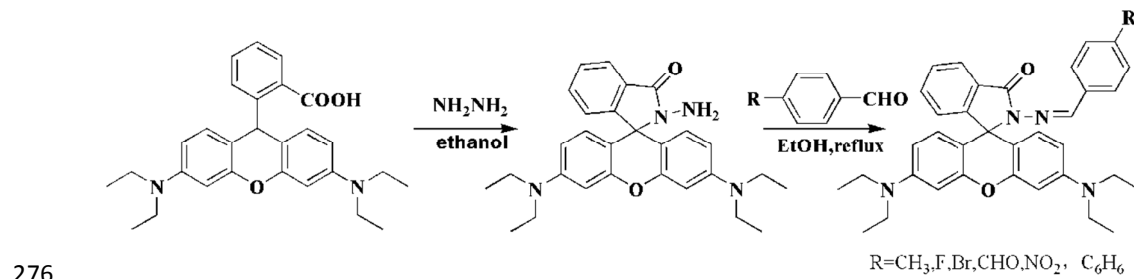
233 This work was supported by the Fundamental Research Funds for the Central  
234 Universities (KYLX15\_0125) and National Major Scientific Instruments and  
235 Equipment Development Projects (2014YQ060773) and A Project Funded by the  
236 Priority Academic Program Development of Jiangsu Higher Education Institutions  
237 (1107047002) and Policy Guidance Program (Research Cooperation)--Prospective  
238 Joint Research Project (BY2016076-02).

239

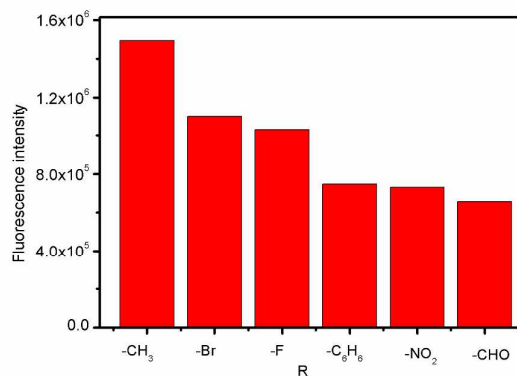
### 240 **References**

- 241 1. Boening, D. W. *Chemosphere* 2000, 40, 1335
- 242 2. Nolan, E. M.; Lippard, S. J. *Chem. Rev.* 2008, 108, 3443
- 243 3. Nolan, E. M.; Lippard, S. J. *J. Am. Soc.* 2003, 125, 14270
- 244 4. Wang, C. *Inorg. Chem.* 2013, 52, 13432
- 245 5. Clarkson, T. W.; Magos, L.; Myers, G. J. *New. Engl. J. Med.* 2003, 349, 1731
- 246 6. Llobet, J. J. *Agr. Food. Chem.* 2003 51 838
- 247 7. Suresh, M. *Org. Lett.* 2008, 10, 3013
- 248 8. Chen, Y.; Han, K. Y.; Liu, Y. *Bioorgan. Med. Chem.* 2007, 15, 4537
- 249 9. Roy, P. *Inorg. Chem.* 2007, 46, 6405
- 250 10. Royzen, M. J. *Am. Soc.* 2006, 128, 3854
- 251 11. Banerjee, A. *Analyst* 2012, 137, 2166
- 252 12. Ding, P. *New. J. Chem.* 2015, 39, 342

- 253 13. Lee, H. Y. *Sensor. Actuat. B-Che.* 2013, 182, 530
- 254 14. Sen, S. *Analyst.* 2012, 137, 3975
- 255 15. Patil, R. *Dal.Trans.* 2014, 43, 2895
- 256 16. Haugland, R. P *The handbook: a guide to fluorescent probes and labeling*  
257 *technologies* 2005,p.52
- 258 17. Huang, J.; Xu, Y. *J. Org.Chem.* 2009, 74, 2167
- 259 18. Suresh, M. *Org. Lett.* 2009, 11, 2740
- 260 19. Zhou, Y. *Org. Lett.* 2009,11,4442
- 261 20. Du, J. *Org. Lett.* 2010, 12 476
- 262 21. McClure, D. S. *J. Chem. Phys.* 1952, 20, 682
- 263 22. Suresh, M.; Ghosh, A. *Chem. Commun.* 2008, 33, 3906
- 264 23. Renzoni, A.; Zino, F.; Franchi,E. *Environ. Res.* 1998, 77, 68
- 265 24. Dujols, V. F.; Ford, A. W.; *J. Am. Soc.* 1997,119, 7386
- 266 25. Yang, X.; Guo,R.; Zhao, Y, B.; *Talanta.* 2002,57, 883
- 267 26. Geng,T.; R, Huang.; Wu D. *RSC Adv.* 2014, 4, 46332
- 268 27. Xiang, Y. *Anal. Chim. Acta.* 2007, 581, 132
- 269 28. Huang, C. Y. *Method. Enzymol.* 1981, 87, 509
- 270 29. Renny, J. S. *Angew. Chem. Int. Edit.* 2013, 52, 11998
- 271 30. Liu, Y, J. *Helv. Chim. Acta.* 2004, 87, 3119
- 272 31. Yan, L. *Spectrochim. Acta. A.* 2016, 155, 116
- 273 32. Liu, X. *J. Tetrahedro.* 2015, 71, 8194
- 274
- 275



Scheme 1. Synthetic route of target compounds.



279

280 Fig.1. Fluorescence intensity (at 580 nm) of L<sub>1-6</sub> (20 μM) in CH<sub>3</sub>CN/H<sub>2</sub>O (1:1, v/v) with the281 presence of Hg<sup>2+</sup> (100 μM) (λ<sub>ex</sub> = 500 nm)

282

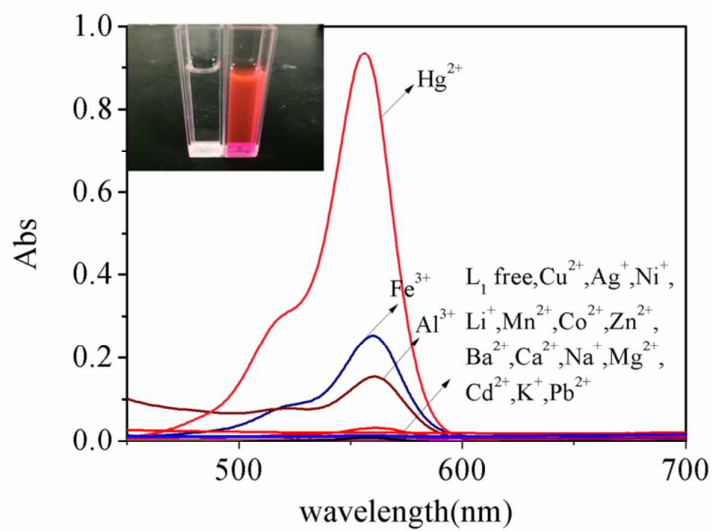
283

Coordination constant						
-R	CH <sub>3</sub>	Br	F	C <sub>6</sub> H <sub>6</sub>	NO <sub>2</sub>	CHO
Coordination constant/M <sup>-1</sup>	3.24E3	2.67E3	2.38E3	2.27E3	3.70E2	2.56E2

284

Scheme 2. The coordination constant of six probes

285



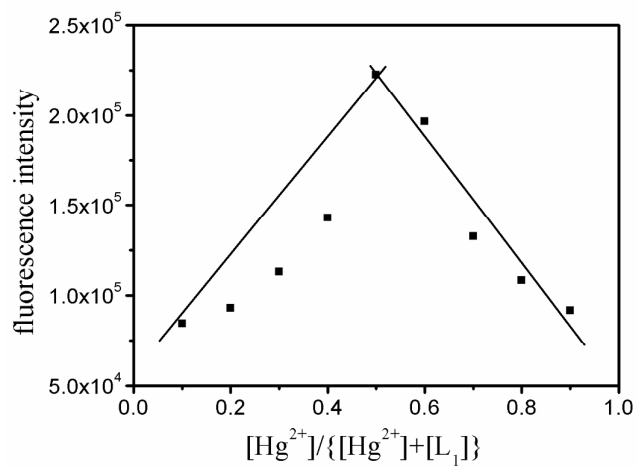
286

287 Fig. 2. Absorbance spectra of  $L_1$  (20  $\mu\text{M}$ ) in  $\text{CH}_3\text{CN}/\text{H}_2\text{O}$  (1:1, v/v) solutions with the presence of

288

10 equiv. of various species.

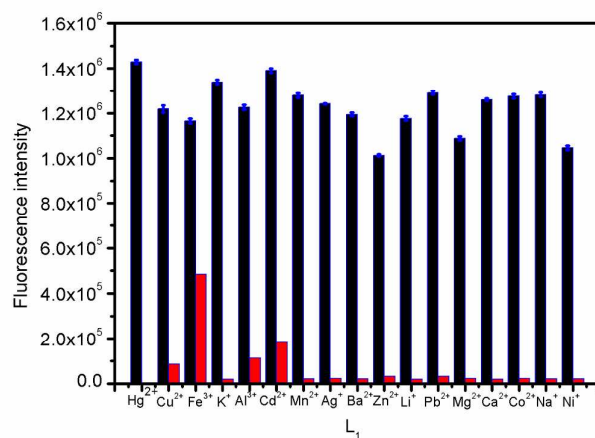
289



290

291 Fig.3. Job's plot of the complexation between  $\text{L}_1$  and  $\text{Hg}^{2+}$ , the total concentration of  $\text{L}_1$  and  $\text{Hg}^{2+}$ 292 is  $20.0 \mu\text{M}$ .

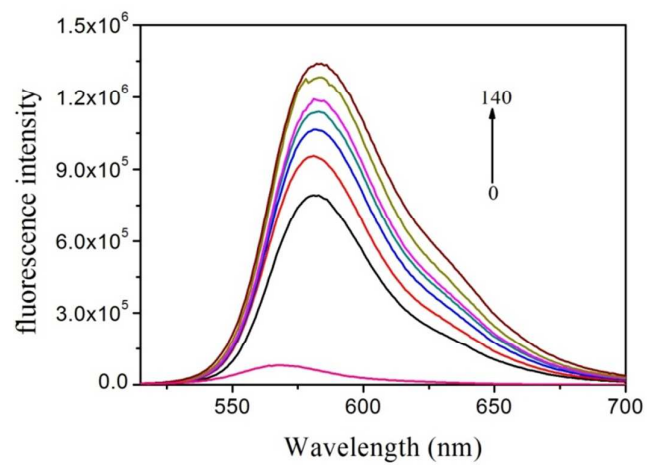
293



294

295 Fig.4. Fluorescence intensity (at 580 nm) of L<sub>1</sub> upon the addition of 20 μM Hg<sup>2+</sup> in the presence296 of 20 μM background metal ions in CH<sub>3</sub>CN/H<sub>2</sub>O (1/1, v/v) (λ<sub>ex</sub> = 500 nm).

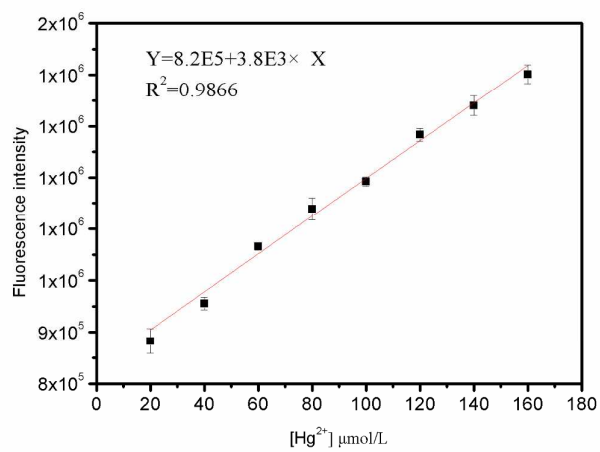
297



298

299 Fig.5(a). The fluorescence intensity (at 580 nm) of compound L<sub>1</sub> (20 μM) as a function of the300 Hg<sup>2+</sup> concentration in CH<sub>3</sub>CN/H<sub>2</sub>O(1:1, v/v) solution ( $\lambda_{ex}$  = 500 nm, slit = 3 nm)

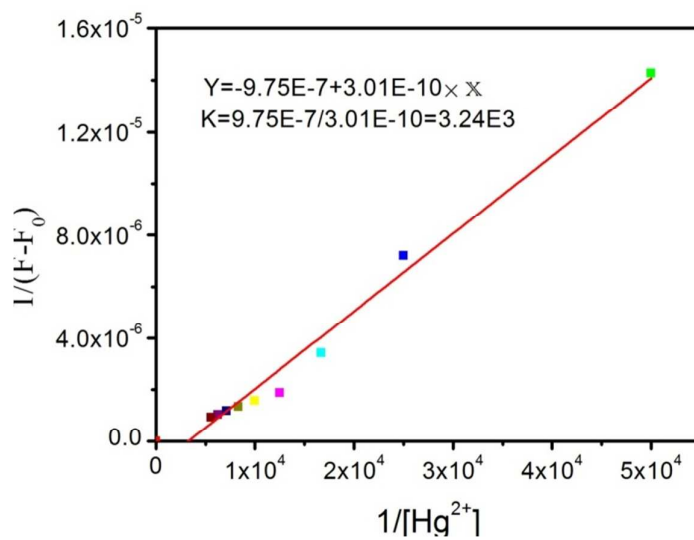
301



302

303 Fig.5(b). Linear relationship of L<sub>1</sub> (20 μM) in CH<sub>3</sub>CN/H<sub>2</sub>O (1:1,v/v) upon addition of different304 amounts of Hg<sup>2+</sup> ions.

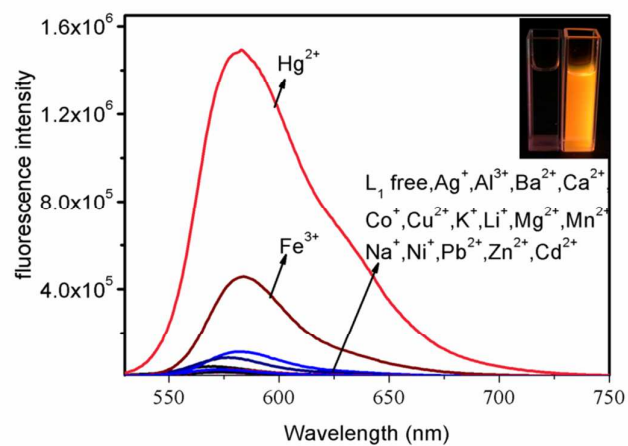
305



306

307 Fig.6. Benesi-Hildebrand plot ( $\lambda_{ex} = 500$  nm) of  $L_1$ , assuming 1:1 stoichiometry for association308 between  $L_1$  and  $Hg^{2+}$  in the solutions.

309



310

311 Fig.7. Fluorescence spectra of L<sub>1</sub> (20 μM) in CH<sub>3</sub>CN/H<sub>2</sub>O (1:1, v/v) with the presence of 10 equiv.312 of various metal ions (λ<sub>ex</sub> =500 nm).

313

314  
315  
316

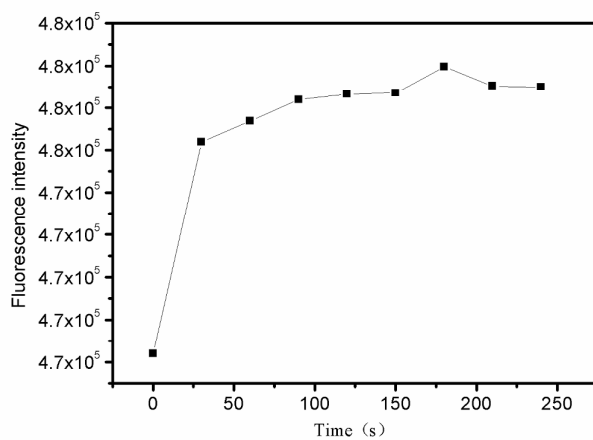
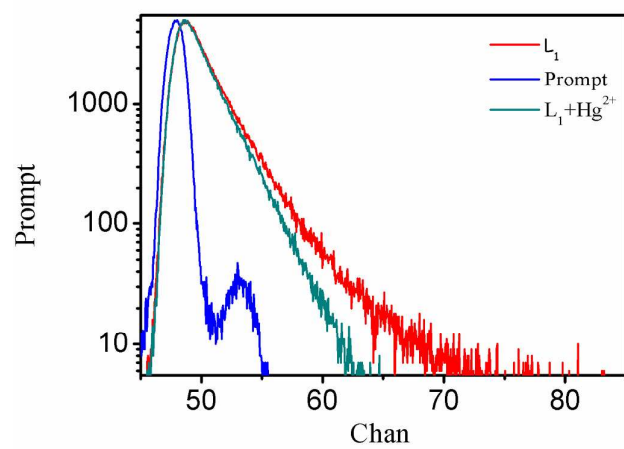


Fig. 8. Effects of time on the reaction of Hg<sup>2+</sup> with L<sub>1</sub>



317

318

Fig.9. Fluorescence decay curves of  $L_1$  and  $L_1 + Hg^{2+}$  in solutions obtained at  $\lambda_{ex} = 500$  nm.

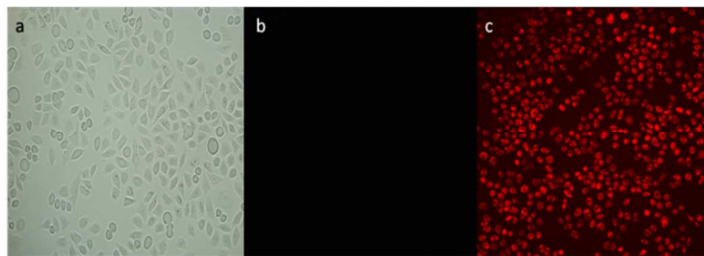
319



320

321 Fig. 10. Photographs of the test kits with L<sub>1</sub> for detecting Hg<sup>2+</sup> in(CH<sub>3</sub>CN/H<sub>2</sub>O = 1:1, v/v) solution322 with different concentrations:(1) 0; (2) 1.0 × 10<sup>-5</sup>M; (3) 1.0 × 10<sup>-4</sup>M; (4) 1.0 × 10<sup>-3</sup>M;(5)1.0 ×323 10<sup>-2</sup>M;(6)1.0 × 10<sup>-1</sup>M.

324



325

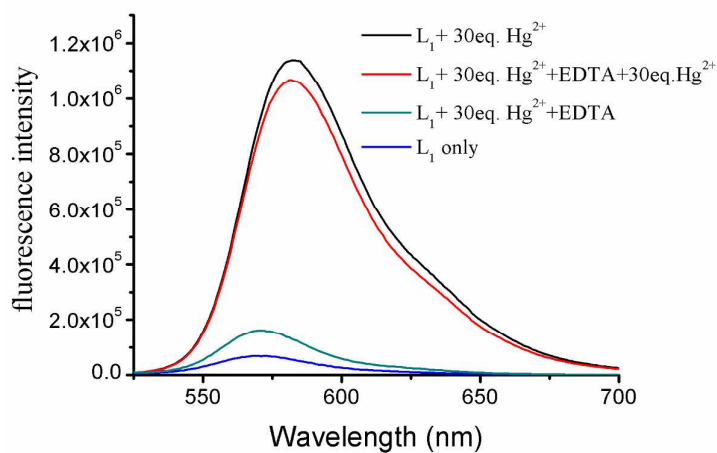
326 Fig.11. Laser confocal scanning microscopy experiments of EC109 cells: (a) Bright-field

327 transmission image. (b) Cells with 10μM solution of L<sub>1</sub> in CH<sub>3</sub>CN–H<sub>2</sub>O (1:1, v/v) for 30 min at

328 25 °C.(c)The staining EC109 cells exposed to L<sub>1</sub> (10μM) for 30 min and then to a CH<sub>3</sub>CN–H<sub>2</sub>O

329 (1:1, v/v) solution of Hg<sup>2+</sup> (10μM) for 30 min.

330



331

332 Fig.12. Fluorescence intensity (at 580 nm) of  $L_1$  (20  $\mu\text{M}$ ) to  $\text{Hg}^{2+}$  in  $\text{CH}_3\text{CN}/\text{H}_2\text{O}$  (1:1,v/v)333 solutions (1) blue line: 10  $\mu\text{M}$   $L_1$  only; (2) red line: 20  $\mu\text{M}$   $L_2$  with 10 equiv.  $\text{Hg}^{2+}$ ; (3) green line:334 20  $\mu\text{M}$   $L_1$  with 10 equiv.  $\text{Hg}^{2+}$  and then addition of 30 equiv. EDTA; (4) black line: 10  $\mu\text{M}$   $L_1$  with335 10 equiv.  $\text{Hg}^{2+}$  and 30 equiv. EDTA then addition of 10 equiv.  $\text{Hg}^{2+}$  ( $\lambda_{\text{ex}} = 500 \text{ nm}$ ).

336

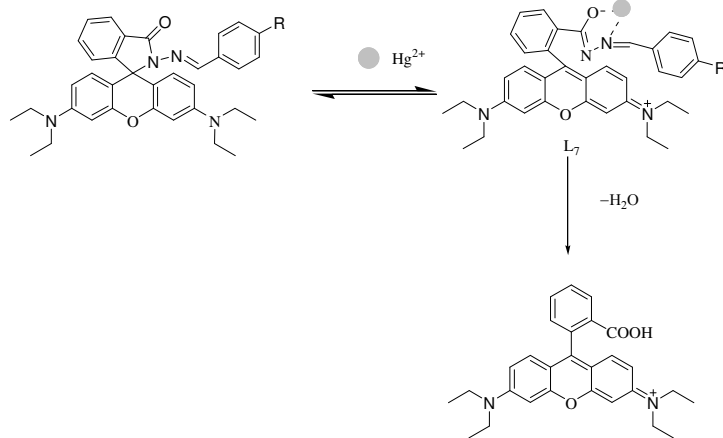
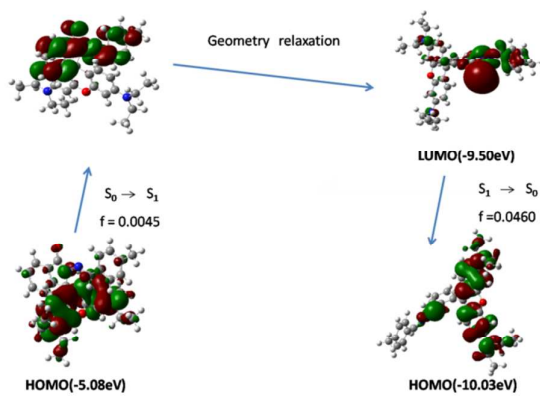


Fig.13. Possible sensing mechanism of  $L_{1-6}$  with  $Hg^{2+}$

337

338

339



340

341

Fig.14. Theoretical molding of the absorption of  $L_1$  without and with  $Hg^{2+}$  at the TDDFT level.